Final Progress Report for Collaborative Research: Aging of Black Carbon during Atmospheric Transport: Understanding Results from the DOE's 2010 CARES and 2012 ClearfLo Campaigns

Award No. DE-SC0010019 (MTU)/ DE-SC0010121 (CMU)

Principal Investigator:
R Subramanian
Research Scientist, Department of Mechanical Engineering, Carnegie Mellon University
5000 Forbes Ave, Pittsburgh, PA 15213
Telephone: 412-268-3850
E-mail: subu@cmu.edu

Co-Principal Investigator:
Claudio Mazzoleni
Associate Professor, Department of Physics, Michigan Technological University
1400 Townsend Drive, Houghton, MI 49931
Telephone: 906-487-1226
E-mail: cmazzoleni@mtu.edu

Unfunded Collaborators:
Arthur J. Sedlacek
Brookhaven National Laboratory

Rahul Zaveri
John Shilling
Duli Chand
Pacific Northwest National Laboratory

Manvendra Dubey
Allison C. Aiken
Los Alamos National laboratory

Report Date: August 31, 2016
Report Activities Period: March 1, 2015 – May 31, 2016

Summary

Over the course of this project, we have analyzed data and samples from the CARES and ClearfLo campaigns, as well as conducted or participated in laboratory experiments designed to better understand black carbon mixing state and climate-relevant properties. The laboratory campaigns took place at PNNL and CMU to study various climate-relevant aerosol properties of different sources of soot mixing with secondary organic aerosol precursors. The DMT photoacoustic extinctiometers (PAXs) procured by CMU through this grant were deployed for these experiments, as well as experiments characterizing the optical properties of cookstove soot emissions at Colorado State University (CSU). Results from some of these activities were summarized in the previous progress report. This final report presents the manuscripts that have been published (many in the period since the last progress report), lists presentations at different conferences based on grant-related activities, and presents some results that are likely to be submitted for publication in 2016.

Publications based on ASR-funded activities

1. Swarup China, Gourihar Kulkarni, Barbara V Scarnato, Noopur Sharma, Mikhail Pekour, John E Shilling, Jacqueline Wilson, Alla Zelenyuk, Duli Chand, Shang Liu, Allison C Aiken, Manvendra Dubey, Alexander Laskin, Rahul A Zaveri, and **Claudio Mazzoleni** (2015). "***Morphology of diesel soot residuals from supercooled water droplets and ice crystals: implications for optical properties***." Environmental Research Letters, 10, 114010 http://iopscience.iop.org/article/10.1088/1748-9326/10/11/114010
2. Georges Saliba, **R. Subramanian**, Rawad Saleh, Adam T. Ahern, Eric M. Lipsky, Antonios Tasoglou, Ryan C. Sullivan, Janarjan Bhandari, **Claudio Mazzoleni,** and Allen L. Robinson (2016). "***Optical properties of black carbon in cookstove emissions coated with secondary organic aerosols: Measurements and modeling.***" Aerosol Science & Technology, http://dx.doi.org/10.1080/02786826.2016.1225947
3. Adam T. Ahern, **R. Subramanian**, Georges Saliba, Eric M. Lipsky, Neil M. Donahue, and Ryan C. Sullivan (2016). "***Effect of secondary organic aerosol coating thickness on the real-time detection and characterization of biomass burning soot by two particle mass spectrometers.***" Atmospheric Measurement Techniques Discussions, http://www.atmos-meas-tech-discuss.net/amt-2016-201/
4. Janarjan Bhandari, Swarup China, Timothy Onasch, Andrew Lambe, Lindsay Wolff, Paul Davidovits, Eben Cross, Adam Ahern, Manvendra Dubey, Claudio Mazzoleni (2016). "***Effect of thermodenuding on the structure of nascent flame soot aggregates.***" Atmospheric Measurement Techniques Discussions.
5. Shang Liu, Allison C. Aiken, Kyle Gorkowski, Manvendra K. Dubey, Christopher D. Cappa, Leah R. Williams, Scott C. Herndon, Paola Massoli, Edward C. Fortner, Puneet S. Chhabra, William A. Brooks, Timothy B. Onasch, John T. Jayne, Douglas R. Worsnop, Swarup China, Noopur Sharma, **Claudio Mazzoleni**, Lu Xu, Nga L. Ng, Dantong Liu, James D. Allan, James D. Lee, Zoë L. Fleming, Claudia Mohr, Peter Zotter, Sönke Szidat, and André S. H. Prévôt (2015). "***Enhanced light absorption by mixed source black and brown carbon particles in UK winter.***" Nature Communications, 6, 8435 doi: 10.1038/ncomms9435
6. Gourihar Kulkarni, Swarup China, Shang Liu, Manjula Nandasiri, Noopur Sharma, Jacqueline Wilson, Allison C. Aiken, Duli Chand, Alexander Laskin, **Claudio Mazzoleni**, Mikhail Pekour, John Shilling,

Vaithiyalingam Shutthanandan, Alla Zelenyuk, and Rahul A. Zaveri (2016). "***Ice nucleation activity of diesel soot particles at Cirrus relevant temperature conditions: Effects of hydration, secondary organics coating, soot morphology, and coagulation***." Geophysical Research Letters, DOI: 10.1002/2016GL068707

7. Chakrabarty, R. K.*, Beres, N. D., Moosmüller, H., China, S., **Claudio Mazzoleni**, Dubey, M. K., Liu, L., and Mishchenko, M. I. (2014). "***Soot superaggregates from flaming wildfires and their direct radiative forcing***." Scientific Reports, 4, 5508.
8. Scarnato, B.*, China, S., K. Nielsen, and **Claudio Mazzoleni** (2015). "***Perturbations of the optical properties of mineral dust particles by mixing with black carbon: A numerical simulation study.***" Atmos. Chemistry and Physics Discussion 15: 2487-2533.
9. Fast, J. D., Allan, J., Bahreini, R., Craven, J., Emmons, L., Ferrare, R., Hayes, P. L., Hodzic, A., Holloway, J., Hostetler, C., Jimenez, J. L., Jonsson, H., Liu, S., Liu, Y., Metcalf, A., Middlebrook, A., Nowak, J., Pekour, M., Perring, A., Russell, L., Sedlacek, A., Seinfeld, J., Setyan, A., Shilling, J., Shrivastava, M., Springston, S., Song, C., **Subramanian, R.**, Taylor, J. W., Vinoj, V., Yang, Q., Zaveri, R. A., and Zhang, Q. (2014). "***Modeling regional aerosol and aerosol precursor variability over California and its sensitivity to emissions and long-range transport during the 2010 CalNex and CARES campaigns.***" Atmos. Chem. Phys., 14, 10013-10060, doi:10.5194/acp-14-10013-2014

The following manuscripts are currently being prepared based on the results presented briefly in this report, with submission expected in 2016:

R Subramanian, Janarjan Bhandari, Swarup China, Noopur Sharma, Rahul Zaveri, and **Claudio Mazzoleni**. "***Mixing State of Black Carbon during CARES 2010: Insights from the SP2 and SEM analysis.***" In preparation for Atmospheric Chemistry and Physics.

Noopur Sharma, Swarup China, Janarjan Bhandari, Kyle Gorowski, Manvenda Dubey, Rahul Zaveri, **Claudio Mazzoleni**. "***Links between physical properties of secondary organic aerosol and internal mixing state of soot particles during the Carbonaceous Aerosols and Radiative Effects Study.***" In preparation for Geophysical Research Letters.

Students and postdoctoral researchers funded by this grant

1. Noopur Sharma (PhD in Atmospheric Sciences, MTU, Fall 2015)
2. Giulia Girotto (MS in Civil and Environmental Engineering, University of Trento, Italy, Winter 2016). Funded as a visiting student for ~6 months while working at MTU.
3. Janarjan Bhandari (current graduate student in the PhD program in Atmospheric Sciences at MTU). Partially supported
4. Swarup China: Postdoctoral researcher.

Conference presentations since February 2015

1. **R. Subramanian**, Janarjan Bhandari, Noopur Sharma, Swarup China, Claudio Mazzoleni, Rahul Zaveri (2016). "***CARES 2010: Diurnal Variation in the Mixing State of Black Carbon Aerosols in Sacramento, CA***." AAAR 35th Annual Conference.
2. **Claudio Mazzoleni**, China, S., Scarnato, B., Sharma, N., Bhandari, J., Mazzoleni, L. R., Fialho, P., Facchini, C., Decesari, S., Gilardoni, S., Zanca, N., European Geophysical Union General Assembly

(2016). "***The Morphology of Atmospheric Aerosol and Some Implications.***" European Geophysical Union, Vienna.

3. **R. Subramanian**, Antonios Tasoglou, Adam Ahern, Eric Lipsky, Christian L'Orange, Kelsey Bilsback, Brooke Reynolds, Kelley Hixson, Jack Kodros, Jeffrey R. Pierce, Michael Johnson, John Volckens, Allen Robinson (2015). "***Shootout at the CSU Corral: Soot Composition and Optical Properties for 23 Cookstove/Fuel Combinations.***" AAAR 34th Annual Conference.
4. Allison C. Aiken, Dubey, M., Liu, S., Zaveri, R., Shilling, J., **Mazzoleni, C.**, China, S., Sharma, N., Zelenyuk, A., Wilson, J., Kulkarni, G., Pekour, M., Chand, D., **Subramanian, R.** (2015). "***Aging Diesel Black Carbon with SOA Coatings and Coagulation to Probe Morphology-dependent Aerosol Absorption Enhancements (Eabs)***." AAAR 34th Annual Conference.
5. Girotto, G., China, S., Aiken, A., Huempfner, R., Gorkowski, K., Dubey, M., and **Mazzoleni, C.** (2015). "***Morphology, mixing state and aging of biomass burning particles***." European Aerosol Assembly, Milan, Italy.
6. Sharma, N., China, S., Zaveri, R., Shilling, J., Pekour, M., Wilson, J., Zelenyuk-Imre, A., Ryan Moffet, R., Moffet, R., Gilles, M., Liu, S., Aiken, A., Dubey, M., Chand, D., Kulkarni, G., Sedlacek, A., **Subramanian, R.**, Onasch, T., Laskin, A., **Mazzoleni, C.** (2015). "***Condensation of secondary organic aerosol on soot seed: effect of relative humidity.***" International Conference on Carbonaceous Particles in the Atmosphere, Berkeley, CA.

Research progress since last progress report

In the following pages, we focus on research results that have not yet been published or submitted for publication, and are included in publications being prepared for submission later this year.

The use of SP2 coating indicators to describe BC mixing state: Lab studies at CMU

The SP2 scattering and incandescence signals can be combined to provide information about the BC mixing state, either using the "incandescence lag" (Moteki and Kondo 2007; Moteki et al. 2007; Subramanian et al. 2010) or by determining the particle optical diameter using an extrapolation (Gao et al. 2007) or derivative (Moteki and Kondo 2008) technique. The incandescence lag (Figure 1) is the gap between the peaks of the scattering signal and the incandescence signal. If there is no significant coating on the BC core, the scattering signal is dominated by the BC particle, and peaks when the particle incandesces and evaporates; thus, the incandescence lag is zero, and the BC particle is classified as "thinly-coated." If there is a significant non-BC coating, as the BC particle absorbs light and heats up, the non-BC coating evaporates, and the scattering signal peaks well before the moment of incandescence (which is almost an instantaneous event.) Positive incandescence lags of 2-4 μs are considered to indicate thickly-coated, internally mixed BC (Subramanian et al. 2010). More recently, Sedlacek and co-workers have also observed negative lag-times – a significant scattering peak appearing after the incandescent peak – though the prevalence of these negative lag-time events is dependent on the SP2 operating conditions, including sampling flow rates and laser power (Sedlacek et al. 2012, 2015).

We conducted lab studies at CMU, injecting size-selected cookstove BC into a 2 m^3 chamber, and gradually coating it with α-pinene SOA (more details in Saliba et al. 2016 and Ahern et al. 2016.) The data from one of these experiments is shown in Figure 2, which shows the increase in particle mobility size from the nascent stage through two subsequent coating stages. Note that the BC mass concentration gradually decreases as particles are lost to the walls after the initial injection, as shown by the SP2 BC mass time-series.

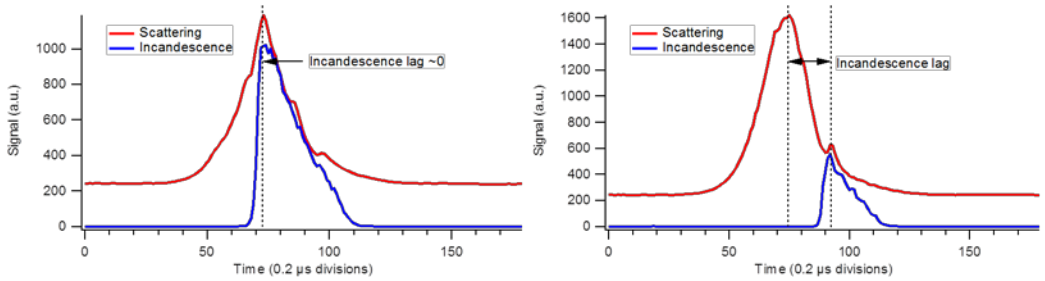

Figure 1: SP2 incandescent and scattering signals for individual particles showing thinly-coated BC (incandescent lag zero, left) and thickly-coated BC (incandescent lag 3-4 µs, right.)

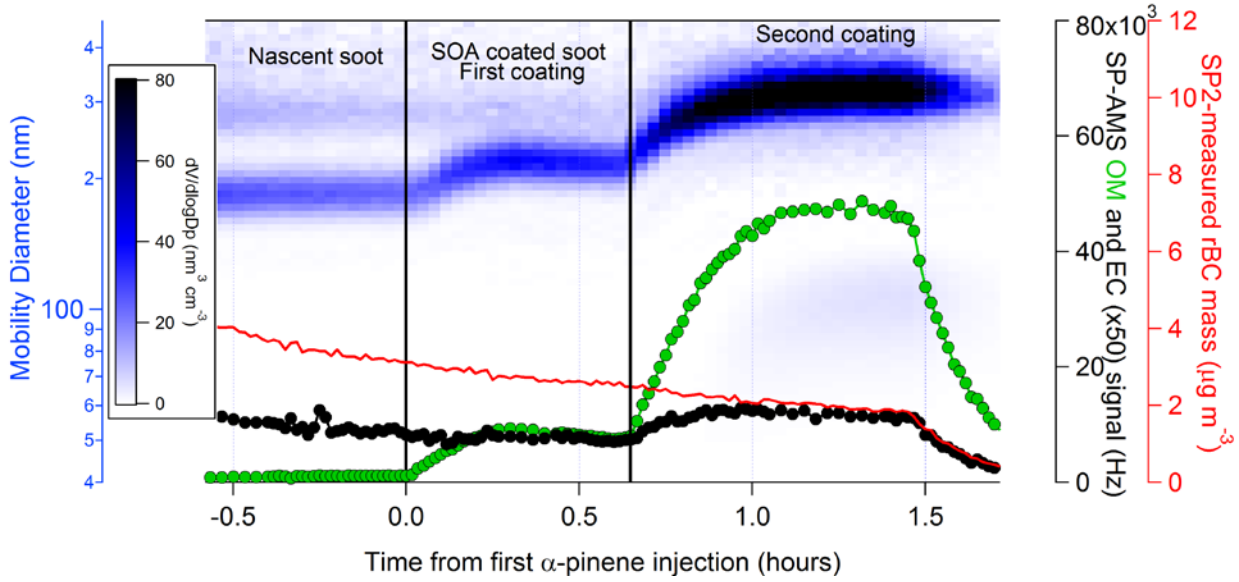

Figure 2. Monodisperse wood-burning cookstove soot particles were injected into a 2 m^3 Teflon bag, followed by two successive injections of α-pinene and ozone, resulting in ozonolysis to produce SOA coatings on the BC cores. Particle growth is evident in the volume-weighted SMPS mobility size distribution (blue-black, top) and the SP-AMS measured OM (green circles) and rBC (black circles) ion signal as a function of time. SP2 rBC mass measurements (red line) reveal the steady decay of soot-particle mass concentration due to chamber wall loss, followed by greater loss when we purged the chamber at t > 1.5 hours. (The SP-AMS "EC" response increases despite wall losses because of an instrument artifact in the SP-AMS; see Ahern et al. 2016 for more details.) This experiment was conducted for three different nascent soot mobility sizes.

Figure 3 shows a time-series of the SP2 BC mass, the SMPS modal diameter, and the fraction of BC aerosols with positive lag time (>1.5 us) and the fraction with negative lag time (<-1.5 µs) during one of these lab experiments. As the BC cores are increasingly coated, we see initial increases in the "thickly-coated" fraction of BC based positive lag-time, but also in the fraction of BC with negative lag-time (1:00 PM to ~2:30 PM). However, as the BC core gets very thickly coated (SMPS modal diameter ~380 nm compared to the nascent mobility diameter of ~220 nm), the "thickly-coated" fraction of BC based on positive lag-time falls to zero, while over 90% of BC shows high negative lag-times. While we did not

collect SEM samples during this experiment, given the gradual coating of the BC cores, we expect the thickly-coated BC cores have a core-shell structure. These lab results indicate that high values of both positive and negative lag can indicate BC cores with significant amounts of associated non-BC material.

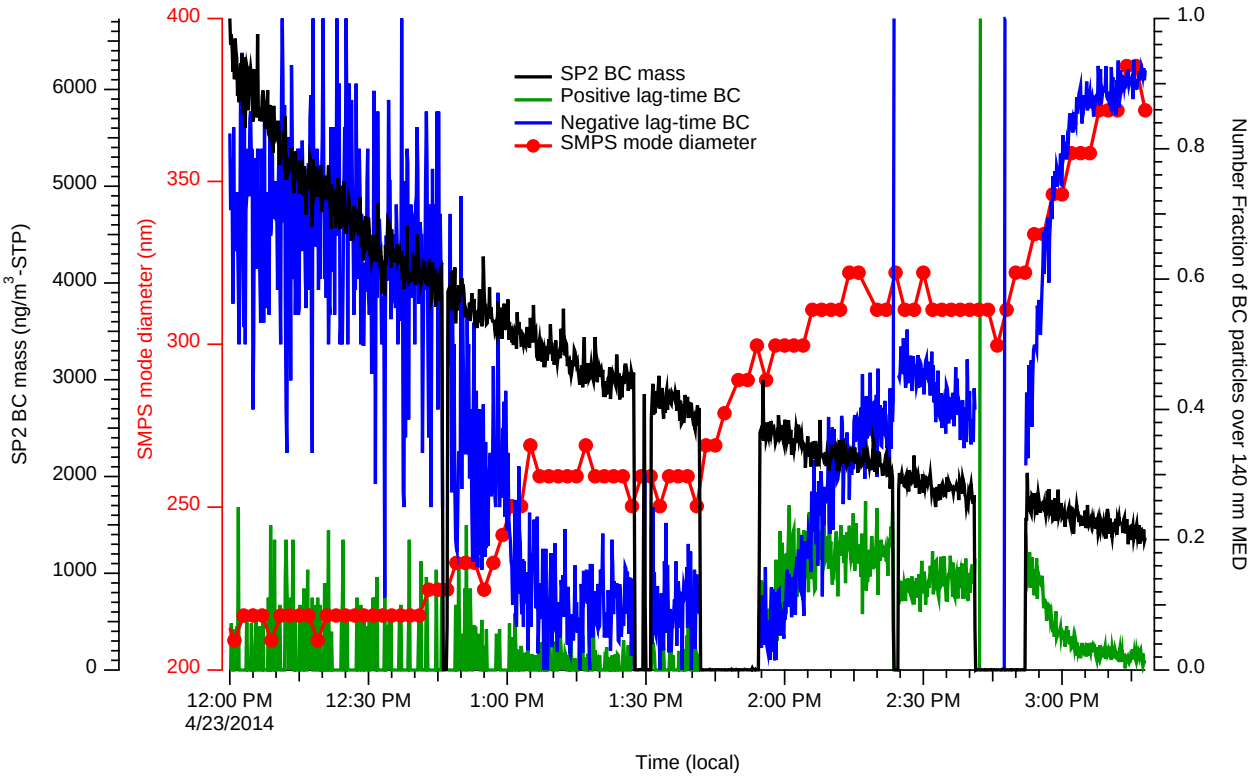

Figure 3: Lab experiments at CMU show that as BC cores are progressively coated with α-pinene SOA (indicated by the increasing SMPS mode diameter), the fraction of BC particles with a negative lag time over 2 µs increases till it reaches ~100%. The nascent soot mobility size in this experiment was 220 nm. The negative lag-time fraction is high before 1 PM because few BC cores are above the SP2's scattering detection limit, as indicated by the noisy data.

The use of SP2 coating indicators to describe BC mixing state: Ambient data from CARES

A second method of examining the non-BC coating thickness on BC cores, called leading edge only (LEO) optimization, uses the optical signal from the two scattering detectors in the SP2 to reconstruct the particle optical diameter before the coating volatilizes (Gao et al. 2007.) The leading edge of the scattering signal, before the coating volatilizes, is extrapolated into a full Gaussian, using information on the Gaussian width (a characteristic of the particular SP2 laser) and the Gaussian peak position, which is also the center of the Gaussian SP2 laser. The center of the laser beam, also the Gaussian peak position, is determined using the signal from a second, two-element scattering detector. The gap between the split and the Gaussian peak, a hardware-based constant, is characterized with non-BC particles, for example polystyrene latex (PSL) standards. In our implementation of the LEO optimization method, the reconstructed Gaussian signal is converted into an optical diameter using a look-up table of scattering cross-section based on the particle diameter and the volume fraction of BC. The coating thickness is determined by the difference between the optical diameter and the mass-equivalent diameter (MED) of

the particle BC mass from the incandescent signal. The LEO optimization method has recently been implemented in our SP2 analysis code (a derivative of the previous Igor-based standard DMT SP2 software, PAPI) in collaboration with Dr Art Sedlacek of Brookhaven National Labs. This new development enables a comparison against the incandescent lag-based BC mixing state information for ambient BC aerosol measured during CARES that have a variety of coating thicknesses, materials, and morphologies, rather than the organic standards (glycerol, oleic acid) and BC surrogates (graphite, Regal Black) employed by Moteki and Kondo (2007) and others.

We now compare the incandescent lag-based mixing state indicators against the LEO-based mixing state information for the same set of BC-containing particles. We seek to determine the equivalence or comparability of these metrics based on ambient data, and will then use an approach that combines the two methods – a weight of evidence approach – to look at BC mixing state during CARES. We examine two weeks of CARES data (June 13-26, 2010 in UTC terms) obtained at the T0 site in an urban environment (Sacramento, CA.) We classify incandescent lags greater than ±2 μs as thickly-coated (based on the observed distribution and to be consistent with previous studies.) In the LEO-based analysis, we use a threshold ratio of optical diameter to BC core diameter (MED) to indicate "thickly-coated" BC. Both sets of data are presented as a fraction of the BC particle number for BC masses larger than 170 nm MED, as uncoated BC particles smaller than this size will likely not have a detectable scattering response (thus, biasing the thickly-coated fraction in favor of coated BC.)

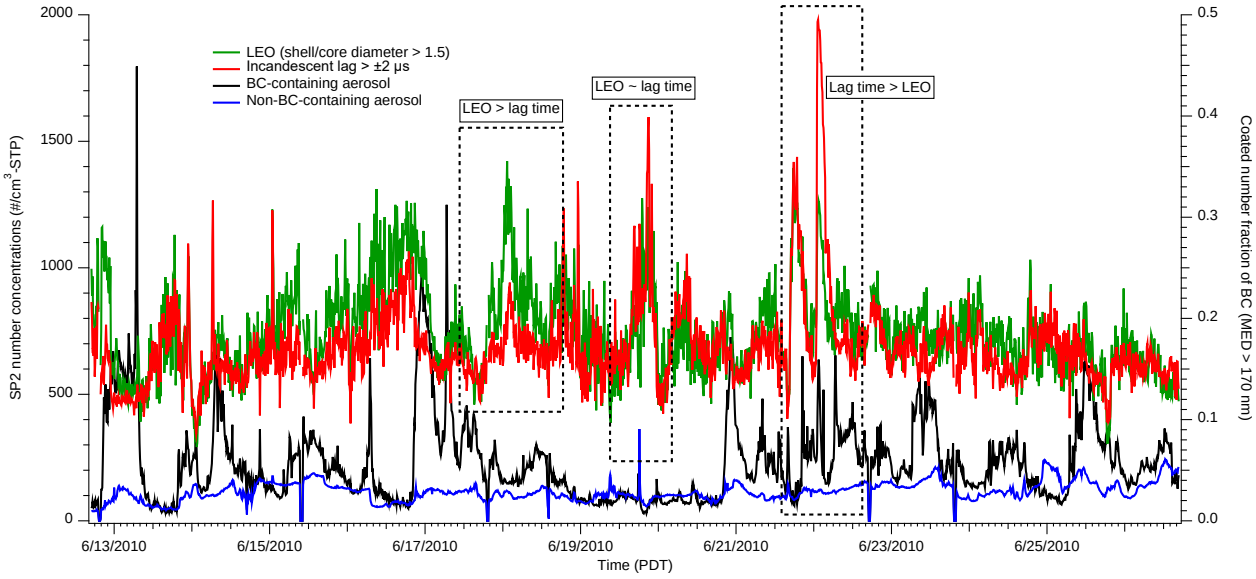

Figure 4: Time-series of SP2 mixing state indicators for the time period from June 12-26, 2010. 10-minute averages starting at 5 PM local time (midnight UTC). Three periods of interest are highlighted to compare and contrast the LEO-based and incandescent lag time approaches used to determine the "thickly-coated" BC fraction in the SP2 data set.

Figure 4 shows a time series of these two ratios, alongside BC and non-BC particle number concentrations observed by the SP2. The first observation is that while most of these "coated BC number fraction" data hover around 20%, there are periods when this fraction reaches 40% to 50%.

Three periods immediately stand out, where the "thickly-coated" BC fraction based on the lag time approach is (a) smaller than; (b) similar to; (c) larger than the LEO-based "thickly-coated" BC fraction. We intend to use other CARES data sets (e.g. SPLAT or AMS) to determine non-BC composition during these periods.

Figure 5 shows scatter plots of different metrics used to describe BC mixing state: the "thickly-coated" BC fraction based on positive lag time and negative lag time, and "thickly-coated" BC fraction based on LEO. Figure 5(A) shows that the negative lag time fraction is always larger than the positive lag time fraction (except for one 10-minute period.) Figure 5(B) shows that the thickly-coated BC fraction based on lag time over +2 μs is much smaller than the LEO-based thickly-coated BC fraction. Thus, use of only the positive lag time threshold to indicate thickly-coated BC would significantly underestimate the fraction of BC aerosols that are thickly-coated.

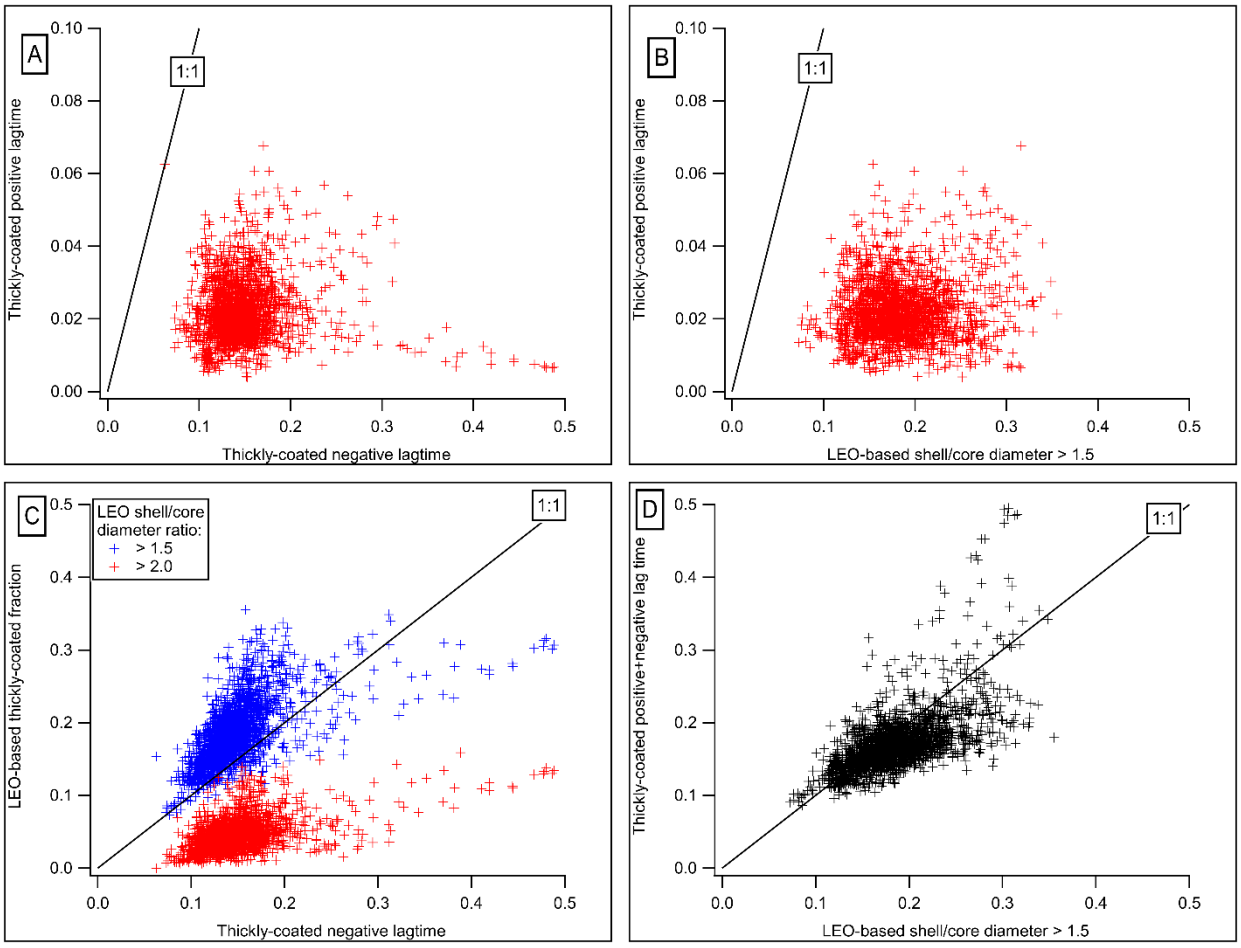

Figure 5: Comparison of different lag time and LEO-based BC mixing state metrics for the CARES T0 data set. 10-minute averages starting at 5 PM local time on June 12, 2010 for two weeks.

Figure 5(C) shows that some high peaks of negative lag time-based thickly-coated BC fractions correspond to high thickly-coated BC fractions based on LEO, whether we use a threshold shell/core diameter ratio of 1.5 or 2.0. Figure 5(D) shows a scatter plot of the two methods, combining the positive

and negative lag times into one metric, and using a minimum shell/core diameter ratio of 1.5. As earlier seen in Figure 4, there is some scatter around the 1:1 line, and there are periods for which one metric or the other gives significantly higher "thickly-coated" BC fractions.

Hence, for the CARES T0 SP2 data set, the positive lag time fraction may indicate some thickly-coated BC, but the negative lag time method is a better indicator of periods with higher thickly-coated BC particles. Sedlacek et al. (2012) reported that periods with high fraction of negative lag time BC are associated with biomass burning smoke and potentially BC-on-edge morphologies. However, based on laboratory experiments with Regal Black (a surrogate for BC) and dioctyl sebacate (an organic compound), Sedlacek et al. (2015) also show the negative lag time fraction can increase with increasing laser power for similarly coated BC particles. The CMU laboratory experiments (Figure 3) with more realistic cook stove soot and α-pinene SOA also showed that negative lag time fraction increases at high shell/core diameter ratios. The SP2 deployed at T0 (DMT serial #02) used a high pump laser power (laser current 3800 mA), though optical alignment may have produced lower intracavity laser power compared to newer SP2s (like the CMU SP2 and the Brookhaven SP2 used by Sedlacek et al.). While we cannot rule out the existence of BC-on-edge morphologies contributing to the negative lag-time fraction observed with the CARES T0 SP2 data set, it is likely that high laser power for the T0 SP2 was a significant contributor to the negative lag times - so long as some non-BC material was associated with the BC core.

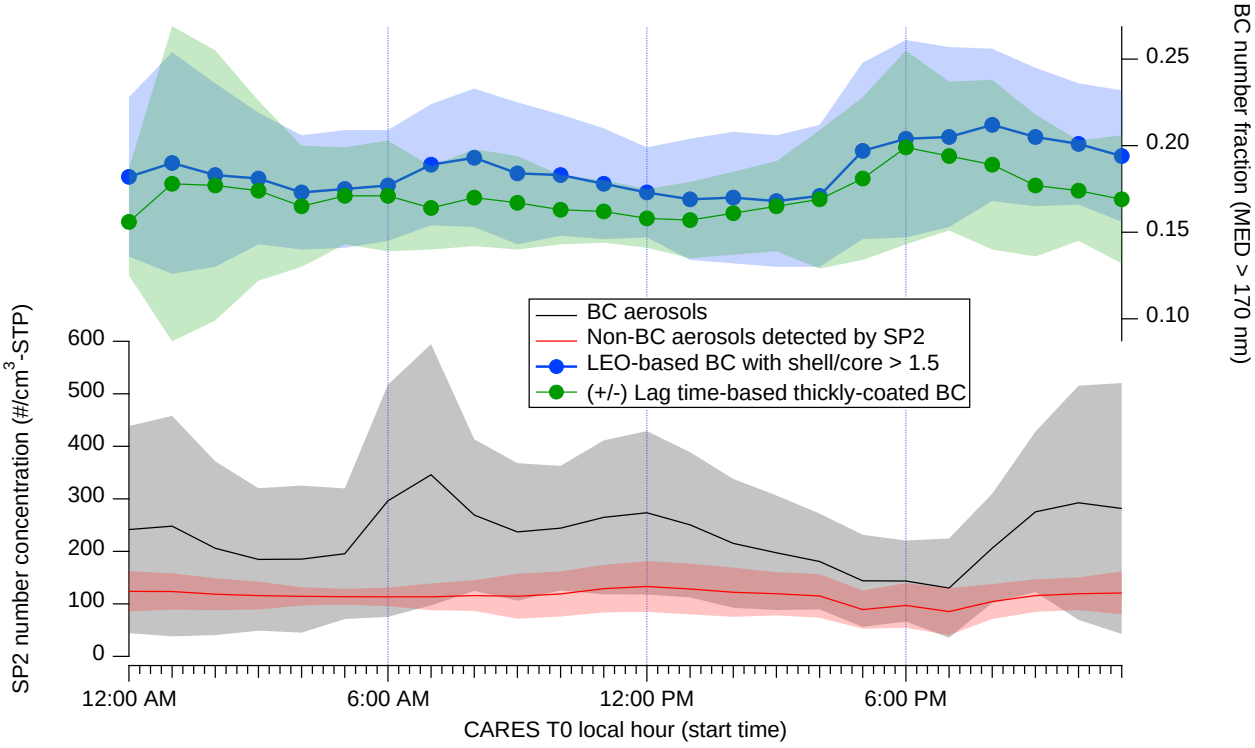

Figure 6: Diurnal trends in SP2-derived BC mixing state indicators at T0 (June 12-26, 2010.) Shaded regions represent ±1 SD of the ten-minute average values in each hour. A BC number peak is observed around 7 AM local time, likely indicating local rush hour emissions. Thickly-coated BC number fraction seems to increase in the afternoon, possibly a result of SOA condensation on BC cores.

Figure 6 shows the average diurnal profile of thickly-coated BC number fraction at T0 for this two-week period, using both lag time and LEO-based methods. Both metrics show an increasing thickly-coated BC number fraction in the late afternoon, starting around 4 PM local time. One caveat is that the BC aerosol observed at T0 is not always the same BC throughout the day; sometimes, it is transported away, which changes the air mass observed. We shall continue to investigate this data set as we prepare the results for publication.

Comparison of SP2 BC mixing state indicators with SEM results

Scanning Electron Microscopy (SEM) provides a visual check of particle mixing state. Figure 7 shows sample SEM images of soot particles analyzed from the CARES campaign, with BC cores classified as "bare soot", "partly-coated soot" (thinly-coated BC), "embedded soot" (heavily coated), and "partially encapsulated soot", signifying a BC-on-edge morphology.

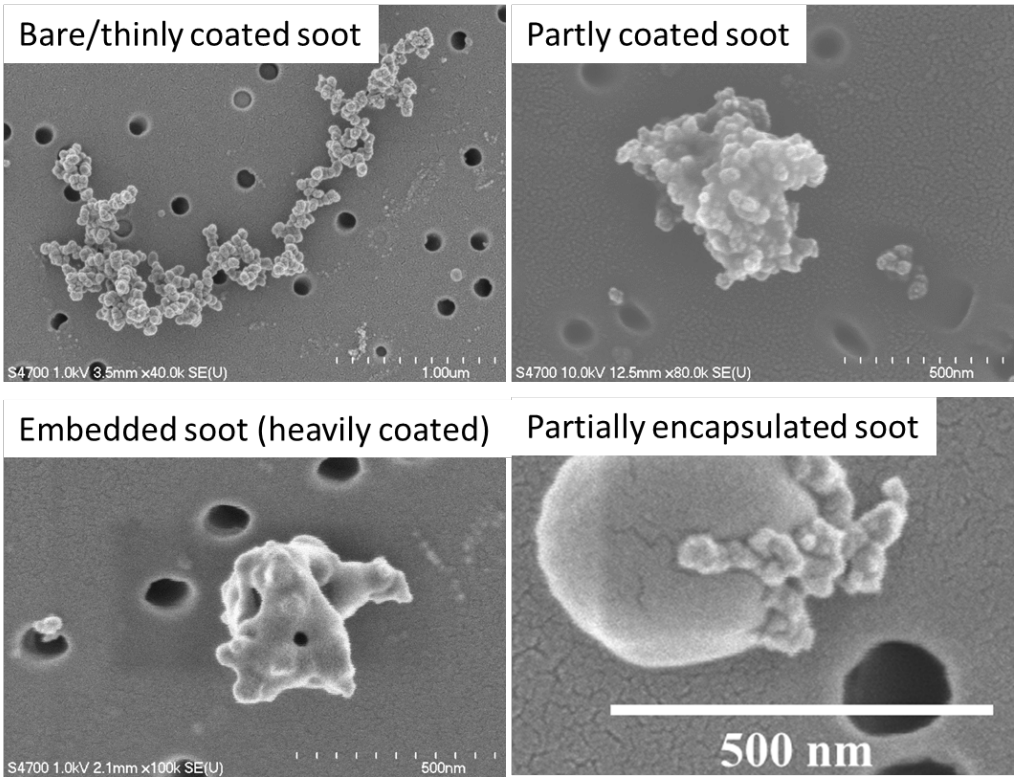

Figure 7: SEM images of soot particles in different mixing states, collected during the CARES campaign.

BC cores collected on SEM substrates on June 25, 2010 were classified as above, and the classifications compared to corresponding SP2-based BC mixing state indicators; the results are shown in Figure 8. We hypothesize that:

(a) SEM's "partly-coated" BC particles have thin coatings that will not be classified as "thickly-coated" BC using the SP2's LEO-based shell/core diameter threshold value of 1.5 we have used so far; hence, we add a coated BC fraction based on a threshold shell/core diameter ratio of 1.1.

(b) Partially-encapsulated or embedded BC cores have substantial non-BC material associated with them, and are more likely to match a higher threshold shell/core diameter ratio of 1.5.

For the June 25, 2010 samples collected at T0, we find that this is indeed the case. The average fraction of SP2 BC particles with an LEO-based shell/core diameter ratio greater than 1.5 is 15%, while the average fraction of embedded or partially-encapsulated/BC-on-edge particles from SEM analysis is 18%. Lowering the LEO-based shell/core diameter threshold to 1.1 increased the coated BC fraction to an average of 61%. This is still uniformly lower than the SEM-based coated BC fraction including the partly-coated BC cores (average 78%). This analysis is complicated by the following factors:

(a) The SP2 classification is based on particles with BC masses over 170 nm MED, while the SEM analysis is based on all observed particles collected on a substrate filter with 100 nm holes. Thus, there is a size mismatch between the two sets of data.
(b) If the BC core is very thickly-coated, the BC core may not be visible in the SEM image, which will bias the embedded (thickly-coated) BC fraction low based on SEM analysis.
(c) SEM analysis is based on 18-47 particles per substrate; at the lower end in particular, the statistical variability could be large as the sample gets less representative.

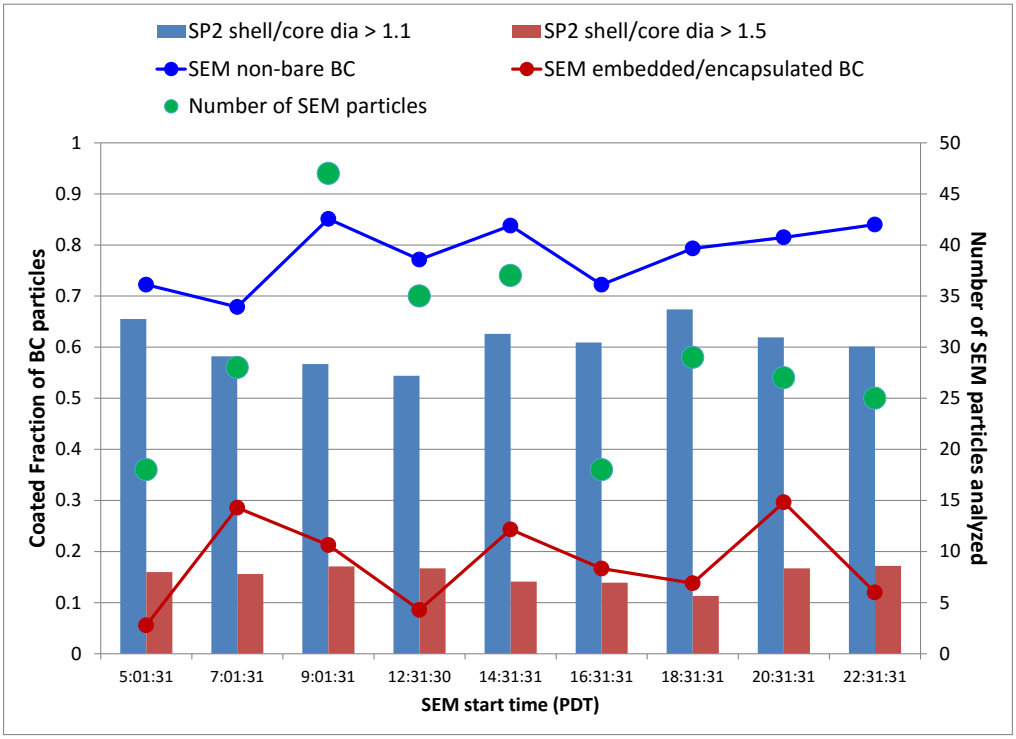

Figure 8: BC mixing state at T0 on June 25, 2010. For the SP2, coated BC fraction refers to particles with BC MED 170 nm or larger and LEO-based shell/core diameter ratios over either 1.1 or 1.5. For SEM, embedded refers to embedded (thickly-coated) particles; encapsulated refers to partially-encapsulated, BC-on-edge structures; "non-bare BC" includes both of these classes and adds partly-coated (thinly-coated) BC cores.

Effect of viscosity of SOA on BC mixing state

We examined the influence of the viscosity of SOA on the evolution of the mixing state of soot likely transported from the Sacramento urban area through a biogenic-influenced environment to the CARES T1 site in Cool, CA. SEM analysis of samples collected at T1 revealed that the observed soot particles were internally (i.e. coated or partially encapsulated) as well as externally mixed. In the external mixture, spherical particles dominated the particle population in all the samples. By imaging spherical particles at high tilt, we observed that a large fraction of spherical and electronically dark particles (as in Figure 9) appeared to be deformed to oblate shapes at impaction, while the remaining electronically bright particles remained nearly spherical.

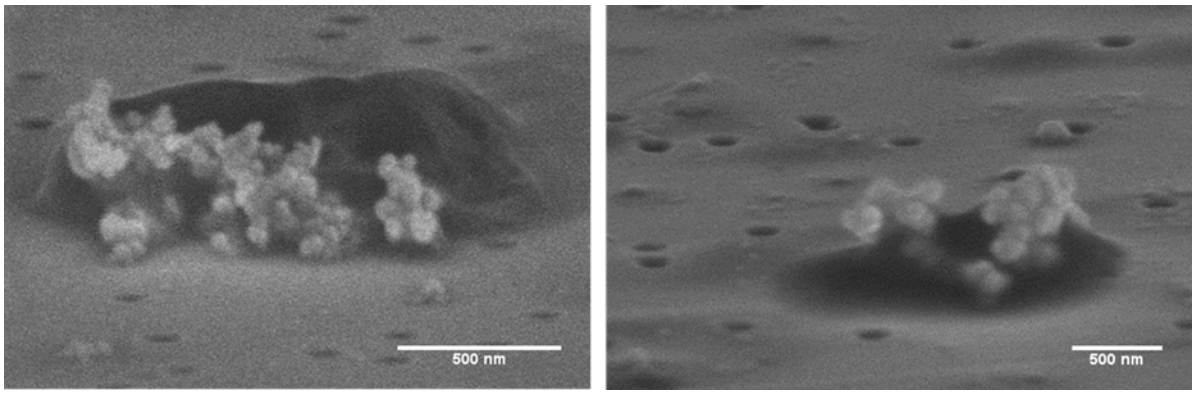

Figure 9: Example of SEM images (obtained at high tilt) of partially encapsulated particles on CARES T1 samples. The soot is intruding the electronically dark, low viscosity host particle.

The deformation of the particles reflects their viscosity or phase state. While the low viscosity particles deformed to non-spherical shapes during impaction, high viscosity particles remained unaffected. The vast majority of the partially-encapsulated soot particles (also called surface-attached soot) were associated with a low viscosity, electronically dark, oblate particle as host. On the other hand, soot mostly remained externally mixed with highly viscous, nearly solid, spherical and electronically bright particles. This suggests that the variable viscosity of SOA particles can be linked to the mixing state of soot resulting from soot-SOA coagulation. The collision of soot with solid/nearly solid particles may not result in coagulation; however, the collision of soot with a particle of lower viscosity results in the formation of surface-attached or partially-encapsulated soot. Coating of soot with organic material is often attributed to condensation of coating material on soot; our study indicates that coagulation of soot with lower viscosity, liquid-like particles can also result in engulfed soot with morphology similar to soot coated through condensation. Therefore, the viscosity of SOA particles plays an important role in determining the mixing state of soot.

SEM analysis of BC aerosols collected during ClearfLo

Two different case studies were analyzed using samples collected at Detling, UK, during ClearfLo. The purpose was to understand the implications of two air masses coming from two different source regions (London and Benelux) on the soot mixing state: 1) air masses coming from the European region called Benelux and 2) air masses coming from the London outskirts. Visiting student Giulia Girotto visually classified 6077 particles based on their morphology into five categories: tar balls, soot, organic matter,

non-soot aggregates and other particles. The most abundant (~55%) was soot. Moderately frequent were spherical (~17%) and near-spherical particles (~20%). Then, Girotto classified 3050 soot particles into 2 main classes: Class a) coated soot and Class b) soot mixed with other kinds of particles, either attached on the surface or only partially encapsulating the soot particle). The most frequent soot (~95%) belonged to Class a). The Class a) soot particles were then subdivided into 3 subcategories depending on the visual amount of coating on the particles (a scale 0 to 3, with 0 indicating minimal coating, and 3 indicating the max amount of coating). The results of this analysis are reported in Figure 10. A summary of some of the quantitative parameters derived from electron microscopy analysis of the soot particles is reported in Table 1.

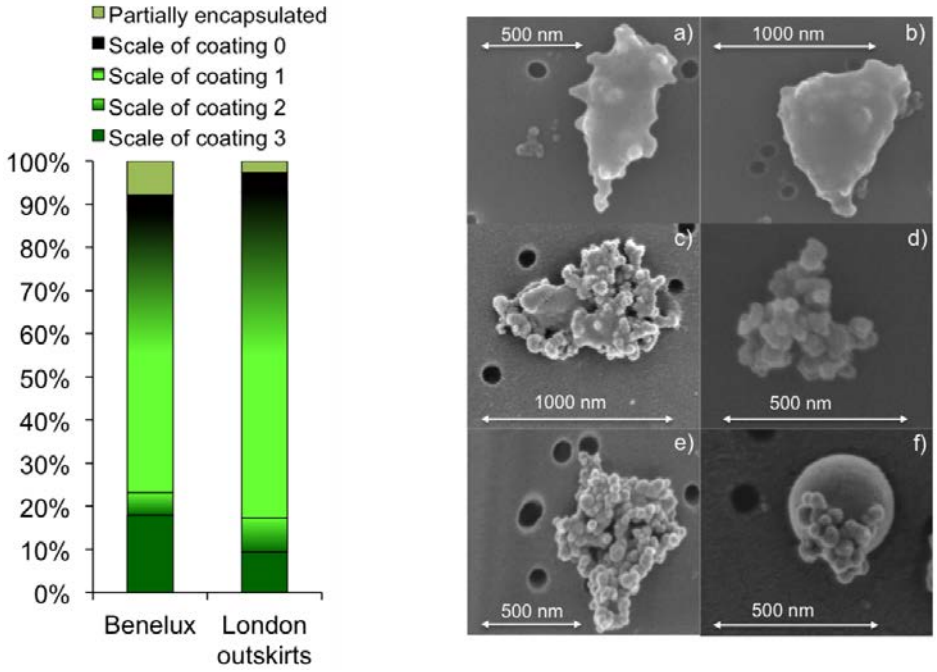

Figure 10: On the left, fraction of different soot types for two transport events (from the Benelux and from the London outskirts) during ClearfLo. On the right, example SEM images showing typical morphologies of soot categorized into five major types of internal mixing state: (a–b) highest scale of coating 3; (c) intermediate scale of coating 2; (d) low scale of coating 1; (e) minimal scale of coating 0; and (f) soot attached with or partially encapsulated by other particles.

Table 1: Averages and standard errors for several morphological parameters for the soot analyzed on samples collected during two transport events (from the Benelux and from London) during ClearfLo. D_{2f} is a 2D estimate of the soot fractal dimension, K_2 is the prefactor, N is the average number of monomers, RN is the roundness, AR is the aspect ratio, L_{max} is the maximum length, d_p the monomer mean diameter and D_{Aeq} the area equivalent diameter of the particle.

Outflow	D_{2f}	k_2	N	RN	Convexity	AR	L_{max} [nm]	d_p [nm]	D_{Aeq} [nm]
Benelux	1.80(0.01)	0.29(0.01)	62(4)	0.46(0.01)	0.78(0.01)	1.61(0.01)	399(9)	57(1)	264(5)
London	1.78(0.02)	0.25(0.01)	63(8)	0.47(0.01)	0.77(0.01)	1.64(0.02)	276(9)	40(1)	178(5)

The effect of thermo-denuding on these particles was also analyzed, showing that thermo-denuding definitely did not remove all the coating from the soot particles. This result can have implications for the validity of estimated absorption and scattering enhancements obtained using a thermo-denuder.

Although these results have not yet been fully synthetized and discussed in a publication, the large statistics and the careful analysis will allow for inclusion of these results in future publications. The analysis is part of the following work:

Giulia Girotto (2016). "*Single Particle Characterization of Atmospheric Carbonaceous Particles Influenced by Biomass Burning."* Master's Thesis, University of Trento, Italy.

Modeling the evolution of BC mixing state during CARES

We are collaborating with PNNL scientists Jerome Fast, Rahul Zaveri, and postdoctoral researcher Ping Pui Ching to evaluate the impact of complex, explicit, observationally-constrained BC mixing state compared to that predicted by internal mixing. Specifically, the BC core size distribution (BC MED) from the SP2 at T0 is used to specify the initial BC size distribution, with the LEO-based coating thickness used to specify the distribution of non-BC coating material (from SPLAT II and AMS data), as the initial conditions to initialize the explicit particle-resolved model, PartMC-MOSAIC. These observationally-constrained particle-resolved simulations are used to examine the atmospheric processing of particles during transport downwind of Sacramento on June 15, 2010, and the associated impacts of mixing state on CCN and aerosol optical properties. In addition to the SP2 deployed at T0 site, the measurement from SP2 installed on the G1 research aircraft is also being used for the PartMC-MOSAIC model output evaluation. This work is currently in progress at PNNL; CMU has provided the necessary SP2 data to PNNL as part of this grant.

References

Ahern, A.T., Subramanian, R., Saliba, G., Lipsky, E.M., Donahue, N.M., and Sullivan, R.C. (2016). "Effect of secondary organic aerosol coating thickness on the real-time detection and characterization of biomass burning soot by two particle mass spectrometers." Atmospheric Measurement Techniques Discussions, http://www.atmos-meas-tech-discuss.net/amt-2016-201/

Gao, R. S., Schwarz, J. P., Kelly, K. K., Fahey, D. W., Watts, L. A., Thompson, T. L., Spackman, J.R., Slowik, J. G., Cross, E. S., Han, J. -H., Davidovits, P., Onasch, T. B. and Worsnop, D. R. (2007). "A Novel Method for Estimating Light-Scattering Properties of Soot Aerosols Using a Modified Single-Particle Soot Photometer." Aerosol Science and Technology, 41:2, 125 – 135, DOI: 10.1080/02786820601118398

Moteki, N. and Kondo, Y. (2007). "Effects of Mixing State on Black Carbon Measurements by Laser-Induced Incandescence." Aerosol Science and Technology, 41:4, 398 – 417, DOI: 10.1080/02786820701199728

Moteki, N. and Kondo, Y. (2008). "Method to measure time-dependent scattering cross sections of particles evaporating in a laser beam." Journal of Aerosol Science 39:348 – 364, doi:10.1016/j.jaerosci.2007.12.002

Moteki, N., Y. Kondo, Y. Miyazaki, N. Takegawa, Y. Komazaki, G. Kurata, T. Shirai, D. R. Blake, T. Miyakawa, and M. Koike (2007). "Evolution of mixing state of black carbon particles: Aircraft measurements over the western Pacific in March 2004." Geophys. Res. Lett., 34, L11803, doi:10.1029/2006GL028943

Saliba, G., Subramanian, R., Saleh, R., Ahern, A.T., Lipsky, E.M., Tasoglou, A., Sullivan, R.C., Bhandari, J., Mazzoleni, C., and Robinson, A.L. (2016). "Optical properties of black carbon in cookstove emissions coated with secondary organic aerosols: Measurements and modeling." Aerosol Science & Technology, http://dx.doi.org/10.1080/02786826.2016.1225947

Sedlacek, A. J., III, E. R. Lewis, L. Kleinman, J. Xu, and Q. Zhang (2012), Determination of and evidence for noncore-shell structure of particles containing black carbon using the Single-Particle Soot Photometer (SP2), Geophys. Res. Lett., 39, L06802, doi:10.1029/2012GL050905

Sedlacek A.J., Lewis, E.R., Onasch, T.B., Lambe, A.T., and Davidovits, P. (2015). "Investigation of Refractory Black Carbon-Containing Particle Morphologies Using the Single-Particle Soot Photometer (SP2)." Aerosol Science and Technology, 49:10, 872-885, DOI: 10.1080/02786826.2015.1074978

Subramanian, R., Kok, G. L., Baumgardner, D., Clarke, A., Shinozuka, Y., Campos, T. L., Heizer, C. G., Stephens, B. B., de Foy, B., Voss, P. B., and Zaveri, R. A. (2010). "Black carbon over Mexico: the effect of atmospheric transport on mixing state, mass absorption cross-section, and BC/CO ratios." Atmos. Chem. Phys., 10, 219-237, doi:10.5194/acp-10-219-2010